

Article

Reduction and Cycloaddition of Heteroalkenes at Ga(I) Bisamide Center

 Vladimir A. Dodonov , Olga A. Kushnerova , Evgeny V. Baranov and Igor L. Fedushkin *

G.A. Razuvaev Institute of Organometallic Chemistry, Russian Academy of Sciences, Tropinina Str. 49, 603137 Nizhny Novgorod, Russia; dodonov@iomc.ras.ru (V.A.D.); kushnerova@iomc.ras.ru (O.A.K.); bar@iomc.ras.ru (E.V.B.)

* Correspondence: igorfed@iomc.ras.ru

Abstract: The reactivity of the complex [(dpp-bian)GaNa(DME)₂] (**1**) (dpp-bian = 1,2-bis[(2,6-diisopropylphenyl)imino]acenaphthene) towards isocyanates, benzophenone, diphenylketene, and 1,2-dibenzylidenehydrazine has been studied. Treatment of **1** with isocyanates led to derivatives of imidoformamide [(dpp-bian)Ga{C(=NPh)₂}-NPh][Na(DME)₃] (**2**), biuret [(dpp-bian)Ga(NCy)₂(CO)₂NCy][Na(DME)] (**3**), or carbamic acids [(dpp-bian)GaN(Cy)C(O)O]₂[Na(THF)(Et₂O)] (**4**), [(dpp-bian)GaC(=NCy)N(Cy)C(O)O][Na(Py)₃] (**5**). Treatment of **1** with 2 equiv. of Ph₂CO resulted in gallium pinacolate [(dpp-bian)GaO(CPh₂)₂O][Na(Py)₂] (**9**), while the reaction of **1** with 2 equiv. Ph₂CCO gave divinyl ether derivative [(dpp-bian)Ga{C(=CPh₂)O}₂][Na(DME)₃] (**10**). Complex **1** treated with 2 equiv. 1,2-dibenzylidenehydrazine underwent [1+2+2] cycloaddition to give C–C coupling product [(dpp-bian)Ga{N(NCHPh)₂(CHPh)₂}[Na(DME)₃] (**11**). When complex **1** was sequentially treated with 1 equiv. of 1,2-dibenzylidenehydrazine and 1 equiv. of pyridine or pyridine-d₅; it gave [1+2+2] cycloaddition product [(dpp-bian)GaN(NCHPh)C(Ph)CN][Na(DME)₃] (**12**). Compounds **2–12** were characterized by NMR and IR spectroscopy, and their molecular structures were established by single-crystal X-ray diffraction analysis.

Keywords: redox-active ligand; low-valent gallium; isocyanate; benzophenone; ketene; azine; cycloaddition



Citation: Dodonov, V.A.; Kushnerova, O.A.; Baranov, E.V.; Fedushkin, I.L. Reduction and Cycloaddition of Heteroalkenes at Ga(I) Bisamide Center. *Reactions* **2024**, *5*, 213–230. <https://doi.org/10.3390/reactions5010009>

Received: 15 December 2023

Revised: 2 February 2024

Accepted: 15 February 2024

Published: 20 February 2024



Copyright: © 2024 by the authors. Licensee MDPI, Basel, Switzerland. This article is an open access article distributed under the terms and conditions of the Creative Commons Attribution (CC BY) license (<https://creativecommons.org/licenses/by/4.0/>).

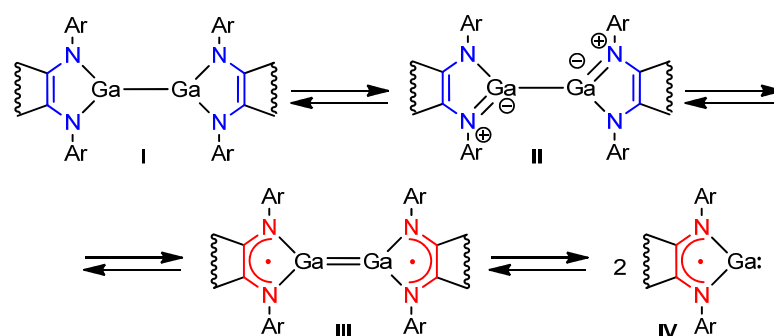
1. Introduction

The discovery of stable carbenes at the end of the 20th century marked a new era in chemistry. These compounds underwent rapid examination and garnered significant favor as ligands for transition metal atoms. Notably, palladium and ruthenium complexes based on N-heterocyclic carbenes have proven effective as catalysts for cross-coupling and olefin metathesis reactions [1,2]. Carbenes themselves are highly reactive and showcase unique properties [3–5], including cycloadditions [6].

Similar carbene-like reactivity is observed in certain compounds of group 13 elements. The entities denoted as RM:, in which M represents gallium or aluminum, have been identified as stable complexes [Cp*Al]₄ (Cp* = C₅Me₅) [7] and [(TMS)₃CGa]₄ (TMS = SiMe₃) [8]. Other spacious ligands, such as amido–imino ligands (e.g., NacNac = (HC(CMeNAr)₂)₂) and aromatic ligands like 2,6-terphenyls, proved to be useful in stabilizing [RM:]_n (where n = 1 or 2, M = group 13 metal) [9–12]. Another class of reactive group 13 species emerges when [R₂M•] (M = group 13 metal) undergo reduction, forming anionic carbenoid [R₂M:][−] species. These anionic species find stabilization through various bisamido ligands, including diaminoxanthene ligands [13], NON-ligands (NON = [O(SiMe₂NAr)₂]^{2−}) [14], SiN^{DIPP} (SiN^{DIPP} = CH₂SiMe₂N(2,6-iPr₂C₆H₃)₂), deprotonated β-diketiminato [15], 1,1,4,4-tetrakis(trimethylsilyl)butane-1,4-diyl [16], and 1,4-diazadiene ligands [17–22]. Additionally, they can be part of cyclic(alkyl)(amino)aluminum anions [23,24].

Molecules of R^{2−}M–MR^{2−}-type exhibit carbene-like behavior if the ligand R is redox-active. Due to the non-innocence of the ligand, these species may exhibit an equilibria R^{2−}M–MR^{2−} ↔ R^{1−}M=MR^{1−} ↔ R^{1−}M (Scheme 1). While controlling electron transfer between

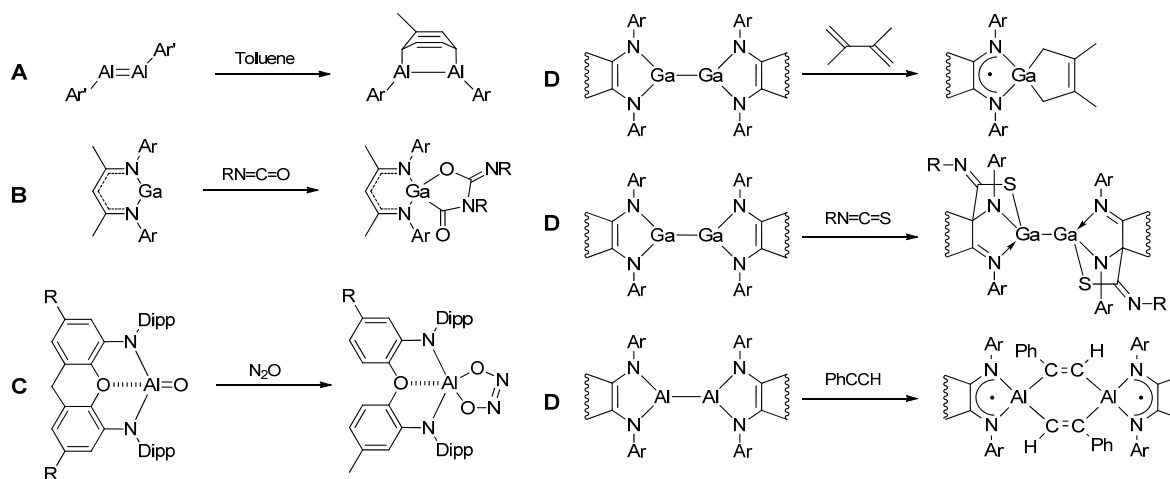
the non-innocent ligand and the metal atom remains a challenge [25,26], the chemical properties of R^2-M-MR^{2-} suggest reactivity resembling heterocyclopentadiene (II) [27,28], dimetallene (III) [29,30], and metallylene (IV) [31,32] types (Scheme 1).



Scheme 1. Structural versatility of R^2-M-MR^{2-} species (R = non-innocent ligand) reflecting various reactivity types.

While the synthesis and structural features of low-valent 13 carbenoid compounds are captivating, their reactivity remains an equally fascinating aspect [33–38]. First, they are good σ -donor/ π -acceptor ligands for transition metal centers [39,40], have high reactivity against organic molecules, can cleave C–C aromatic bonds [41], and insert into robust C–H [16,42–45], C–F, C–O [46], C=N [47], C=S, P=S bonds [48]. Low-valent 13 group compounds were reported to undergo transition metal-like oxidative addition [31,49–51] and reductive elimination [52,53]. This made them environmentally safe candidates to replace expensive transition metal complexes in catalysis [54].

Despite structural and electronic differences, all the aforementioned metallylenes can undergo cycloadditions [55]. Dialumenes, reminiscent of olefins (Scheme 2, A), unveil their intriguing propensity for [2+2] cycloaddition reactions with an array of substrates—ranging from CO_2 [56], olefins, and alkynes [57,58] to unactivated benzene rings [59,60]. Gallium terphenyl dimetallene $ArGaGaAr$ (Ar = 2,6-terphenyl) was reported to react under ambient conditions with ethylene, propene, 1-hexene, and styrene to give 1,4-digallacycloalkanes [61].



Scheme 2. Cycloaddition on 13 group low-valent species.

Meanwhile, RM: species proceed with [2+1] or [4+1] cycloadditions. $[NaCNacAl:]$ reacts with alkynes to form alumacyclopropenes [62], alkenes to form alumacyclopropanes [63,64], and cyclic, acyclic and aromatic dienes [64,65], carbonyl compounds [66], and 1,4-diphosphinine [67]. Anionic aluminum(I) complexes react with 1,3,5,7-cyclooctatetrene [14] or unsaturated hydrocarbons [68]. $[NaCNacGa:]$ undergoes a cycloaddition reaction with

two equivalents of RNCO (R = Ph; 3,5-Me₂C₆H₃) or two equivalents (p-Tol)N=C=N(p-Tol) (Scheme 2, B) [69]. Cycloaddition may occur at polar groups M=E (E = O, S, N(2,6-iPr₂C₆H₃)) [70–74] (Scheme 2, C). Noteworthy examples include cycloadditions of iso(thio) cyanates to monomeric aluminum sulfide [NaCNacAl=S] [48]. At the same time, alumylene oxide $[(\text{NON})\text{Al}=\text{O}]\text{K}_2$ was reported to react with an equivalent of CO₂, PhNCO, or N₂O via a [2+2]-cycloaddition mechanism to produce aluminum carbonate, carbamate or hyponitrite [75]. The structural flexibility of low-valent species containing redox-active ligands leads to a larger scope of cycloaddition reactions, including [4+1]-, [4+2]-, and [2+2+1+1]- cycloaddition [76–78] (Scheme 2, D).

Attempts have been made to apply these concepts, but as of now, the achievements in this area are quite limited, in contrast to applied low-valent surfaces and solid-state chemistry [79,80]. Metallylenes were employed for selective coupling of carbonyl compounds, isocyanates, nitriles, imines, and azides with pyridine [81] or benzophenone [66]. They promoted a facile synthesis of phosphine PH₃ from white phosphorus and ammonia [82]. Alumene's adducts of olefins can undergo a reversible insertion of CO [83]. Benzene was converted into acyclic 1,3,5-triene products at a low-valent aluminum center [84]. Recently, we reported a direct transformation of RN=C=NR to guanidates and iminoguanidates [85,86], activation and modification of CO₂ into carboxylic acid derivatives [87] mediated by gallylene complex $[(\text{dpp-bian})\text{GaNa}(\text{DME})_2]$ (**1**).

Here, we report on novel transformations of RN=C=O, Ph₂C=O, Ph₂C=C=O, N₂O, COS and PhHC=N-N=CHPh at the gallium center of complex **1** and draw certain generalizations regarding the patterns that govern them.

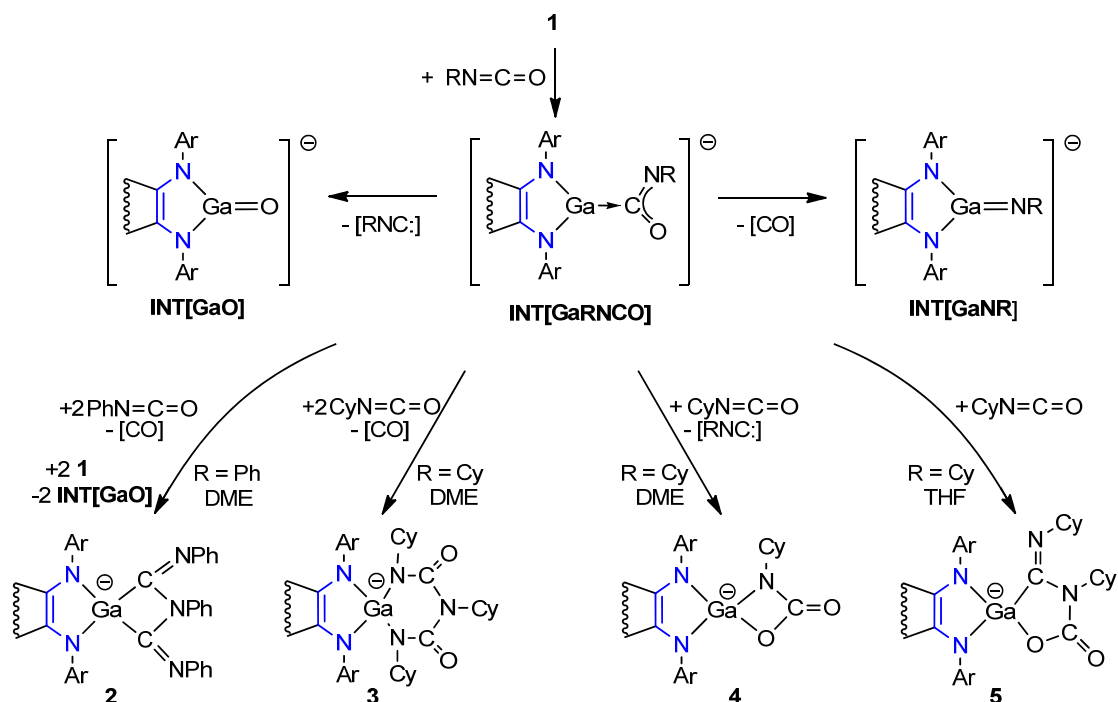
2. Materials and Methods

General procedure for synthesis of **2–12**. All the manipulations with air- and moisture-sensitive compounds were carried out in a vacuum or under argon using the standard Schlenk technique or under an argon atmosphere in a drybox. A solution of **1** equiv. of $[(\text{dpp-bian})\text{GaNa}(\text{DME})_2]$ [88] was prepared in situ by stirring 0.5 equiv. $[(\text{dpp-bian})\text{Ga}]_2$ with 1 equiv. of sodium metal in a relevant ether solvent until the metal completely dissolved. The solution became yellow-green. Then, 1 (or 2) equiv. of heteroalkene was added to the solution. Within a few minutes, the solution's color became green/green-blue. Further crystallization afforded green/green-blue diamagnetic crystals of compounds **2–12**.

Details of synthesis, characterization, X-ray crystal structure determination details, and crystal data are given in the electronic supplementary materials. CCDC 2314238 (**2**), 2314239 (**3**), 2314240 (**4**), 2314241 (**5**), 2314242 (**6**), 2314245 (**7**), 2314246 (**8**), 2314247 (**9**), 2314248 (**10**), 2314249 (**11**) and 2314250 (**12**) contain the supplementary crystallographic data for this paper. These data can be obtained free of charge via ccdc.cam.ac.uk/structures (accessed on 13 December 2023).

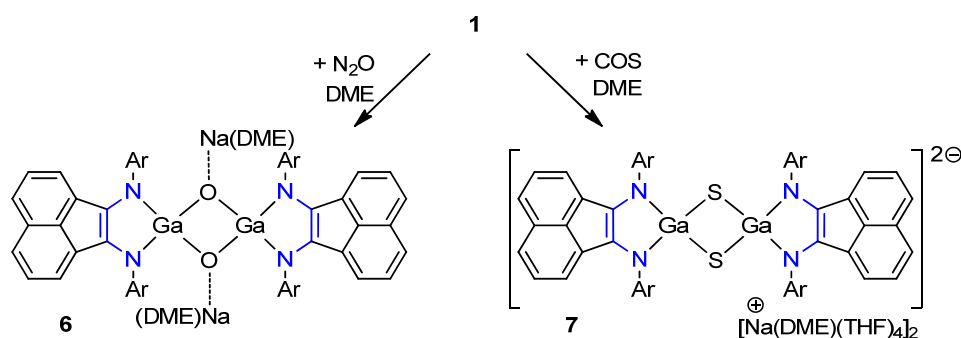
3. Results and Discussion

Metallylene's $[(\text{dpp-bian})\text{GaNa}(\text{DME})_2]$ (**1**) reactivity against isocyanates was tested in three conditions: (1) **1** with 1 equiv. of PhNCO in DME solution, (2) **1** with 1 equiv. of CyNCO in DME solution, and (3) **1** with 2 equiv. of CyNCO in THF solution at 25 °C. A rapid solution color change from yellow-green to green-blue was observed. However, despite similar reaction conditions, the isolated products were strikingly different in each case (Scheme 3). The imidoformamide **2** was isolated from the first reaction, biuret (**3**) and carbamic acid (**4**) derivatives from the second reaction, and carbamic acid (**5**) from the third reaction, respectively. The products appeared to be especially moisture- and air-sensitive crystals of various green-blue tones indicative of dpp-bian^{2-} [31] that were isolated in moderate 11–18% yields. Compounds **3** and **4** were isolated from the same reaction mixture simultaneously.



Scheme 3. Reaction of gallylene **1** with CyNCO and PhNCO to yield complexes **2–5**. Counter ions and acenaphthene parts are omitted for clarity.

Formation of **2–5** can be rationalized through the mechanism suggested earlier for the reaction of **1** with O=C=O [87]. It anticipates the formation of intermediate adduct **INT[GaRNCO]** (Scheme 3). The reaction is followed by the [3+2] or [3+2+2] cycloaddition of a second and a third molecule of isocyanate with concomitant extrusion of isonitrile or CO. Moreover, the intermediate **INT[GaRNCO]** is supposed to have two competitive decomposition pathways to the oxide **INT[GaO]** and the imide **INT[GaNR]**, which are unstable towards dimerization [87]. According to the proposed mechanism, the generation of species **2** should have led to a noticeable amount of **INT[GaO]**, which was well supported by an experiment. A deeper inspection of the reaction mixture of **1** with PhNCO allowed the isolation of green crystals of an **INT[GaO]** dimer, the gallium oxide [(dpp-bian)GaO]₂[Na(DME)₂]₂ (**6**), on top of crystals of complex **2**. The relatively low isolated yields of **2–5** may be attributed to the existence of few energetically close intermediates **INT[GaO]**, **INT[GaNR]**, **INT[GaRNCO]** along with the presence of competitive reaction pathways that, in fact, resulted in a mixture of similar products. Complex **6** was also synthesized by the direct reaction of gallylene **1** with 1 equiv. N₂O (Scheme 4) as green crystals in 66% yield. Spectral characteristics of **6** from both experiments coincided. For the sake of **6** synthesis, compound **1** was also treated with 1 equiv. carbonyl sulfide. That, however, resulted in sulfide **7** as green crystals in 35% yield.

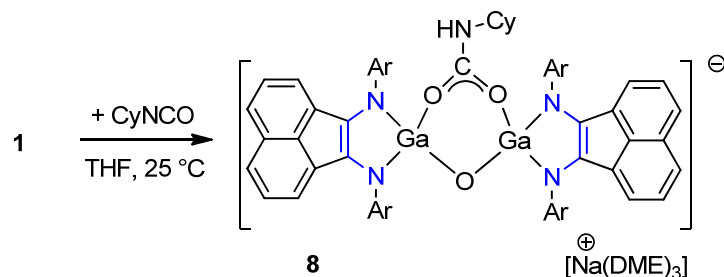


Scheme 4. Reaction of gallylene **1** with 1 equiv. of N₂O and 1 equiv. of COS.

Compounds 2–6 are diamagnetic and produce resolved NMR spectra. Complexes of dpp-bian that have symmetry elements produce a characteristic pattern of the ligand NMR [87]. Likewise, the NMR spectra of a solution of 2 contain a simplified set of signals due to two symmetry planes. Eight methyl groups and four methine groups of iPr are presented by two doublets (δ 0.75, 0.89 ppm, 12H each) and one septet (3.74 ppm, 4H), respectively. Protons of the phenyl group produce signals at 7.56 (2H), 7.25 (2H), 7.01 (4H), 6.78 (4H), 7.06 (1H), and 6.57 (2H) ppm. The GaC(NPh)N carbon atom produces a signal at 152.8 ppm that is similar to 158.1 ppm of azacyclobutane C(=NPh)C(Me₂)N(Ph)C(=NPh) [89]. Compounds 3 and 4 were characterized only by XRD analysis because of very close solubilities. The NMR spectrum of complex 5 demonstrates a simplified signal set due to a symmetry plane. Protons of the methyl and methine groups of iPr give four doublets (6H each) and two septets (2H each). Protons of the naphthalene part appear as two doublets (2H each) at 6.29 and 7.12 ppm and one doublet of doublets (2H) at 6.86 ppm. Protons of methylene groups cyclohexyl substitutes give six multiplets at 2.79 (2H), 1.89 (2H), 1.70 (4H), 1.57 (4H), 1.37 (4H), and 1.18 (4H) ppm. Protons of the methine groups produce two broad singlets (1H each) at 4.82 and 3.54 ppm. Compound 6 is poorly soluble in ether solvents, aggravating its NMR identification. The ¹H NMR spectra of 6 exhibited two doublets (24H each) at 0.96 and 0.86 ppm and one septet (8H) at 3.77 ppm for the protons isopropyl group indicative of three symmetry planes. The reactions from Scheme 3 seem to be unselective; NMR-scale experiments resulted in untrackable mixtures of products.

The IR spectra of the compounds 2–6 support the proposed structures. Compound 2 features a strong C=N absorption band (1640 cm⁻¹). The mixture of 3 and 4 exhibits absorption at 1628 cm⁻¹ and 1602 cm⁻¹, corresponding to C=O and C=N vibrations. The IR spectrum of compound 5 consists of the absorption of 1714 cm⁻¹ and 1661 cm⁻¹, which are characteristics of double C=O and C=N bonds, respectively. No -N=C=O absorption bands were registered in the 2000–2300 cm⁻¹ region.

In a separate experiment, adventitious contact of a reaction mixture of 1 with 1 equiv. CyNCO in THF with air led to the isolation of green crystals of compound [(dpp-bian)GaOC(NHCy)O(O)][Na(DME)₃] (8) in 9% yield (Scheme 5).



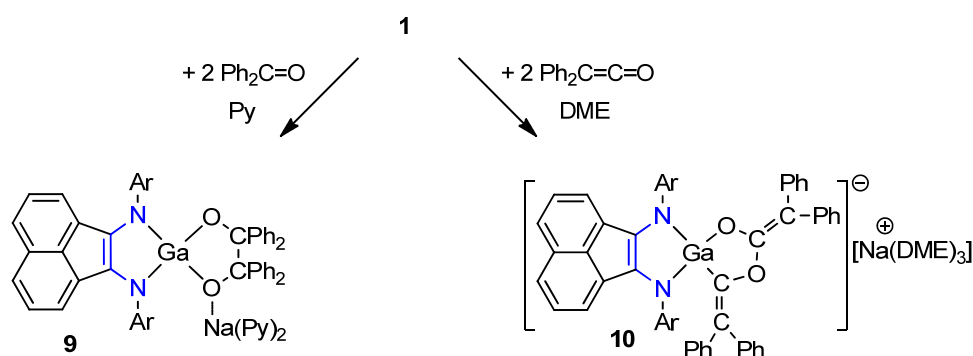
Scheme 5. Reaction of gallylene 1 with 1 equiv. of CyNCO to yield 8.

Complex 8 is diamagnetic but shows no resolved NMR spectra at room temperature, probably due to molecular motion in the cyclohexyl substituent. The spectrum resolution improved at -20 °C (Figure S19). Protons from the isopropyl group produced signals at 1.20, 1.03, 0.74, and 0.71 ppm (12H each) and 3.84 and 3.48 ppm (4H each). Protons of cyclohexyl substitutions appeared at 3.07 (1H), 2.20 (4H), 1.99 (4H), and 1.12 (2H) ppm. Atom H(5) of the imino group presented as a doublet at 5.79 ppm. The IR spectrum of product 8 contains absorption bands corresponding to stretching vibrations of N–H (3364 cm⁻¹) bonds and a carboxyl group (1591 and 1438 cm⁻¹).

Even though the isocyanate oligomerization phenomenon under basic or reductive conditions is known [90,91], and we reported a few isocyanate transformations on the gallium center [27], most of the structures and transformations reported herein are novel. For example, complex 2 is the first metalocycloiminoacylamidine of the main group metal. Three metalocycloiminoacylamidines of the transition metals were characterized, though. They were isolated by the insertion of 2,6-dimethylphenyl isocyanide to the M–N bond of platinu-

mazacyclopropane [(RCN)₂PtC(=NR)NR] (R = 2,6-dimethylphenyl) [92] and transformation of isonitrile in the coordination sphere of iron in the complex [Fe(dppe)(CNR)₄](ClO₄)₂ (R = p-Tol; dppe = 1,2-bis(diphenylphosphino)ethane)) by its treatment with excess KOH [93]. Similarly, complex **3** is the second main group metal biuret to be deposited in the Cambridge Structural Database (CSD) [27]. Isocyanate oligomerizations were reported to give six-member metallacycles on nickel [94], palladium [95], and chromium [96] centers. To the best of our knowledge, the generation of compounds with five-membered metallacycle MC(=NR)C(=O)O, like in complex **5**, is also unprecedented.

To better understand the reactivity of **1** against C=O-containing compounds, it was treated with 2 equiv. of benzophenone or 2 equiv. of diphenylketene. Green crystalline products [(dpp-bian)GaO(CPh₂)₂O][Na(Py)₂] (**9**) (53% yield) and [(dpp-bian)Ga{C(=CPh₂)O}₂][Na(DME)₃] (**10**) (22% yield) were isolated from the reaction mixtures, respectively (Scheme 6).

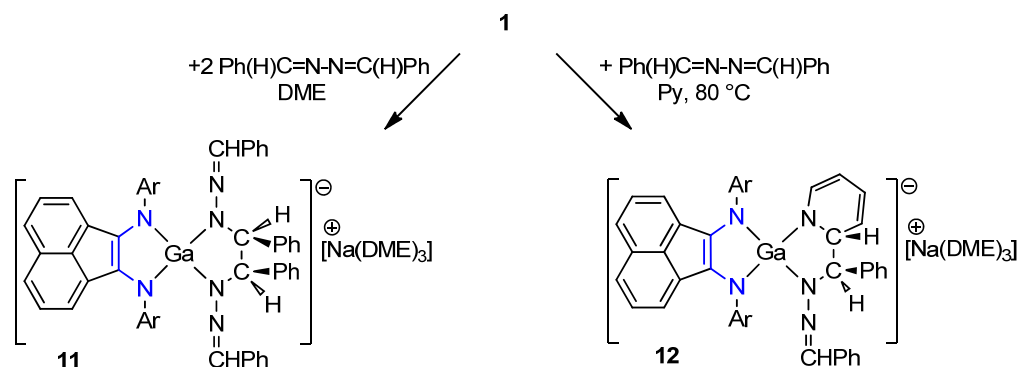


Scheme 6. Reaction of **1** with 2 equiv. of Ph₂CO and with 2 equiv. of Ph₂CCO.

NMR spectra of the compounds **9** and **10** supported their structure. Protons of isopropyl substituents have shown a set of two doublets (12H each) and one septet (4H) associated with two symmetry planes. At the same time, those of **10** produced four doubles and two septets indicative of only one symmetry plane. The chemical shift of the quaternary carbon atom of the pinacolate fragment of δ 88.6 ppm was significantly shifted to a stronger field (cf. δ (¹³C) = 196.5 ppm in Ph₂CO). ¹³C NMR chemical shifts of sp²-hybridized carbon atoms of the galladioxolane fragment (161.1 (OCO), 158.1 (OCGa), 127.6 (Ph₂C=COGa), 88.6 (Ph₂C=CO₂) ppm) are close to those in the phosphorus derivative [PhPOC(=CPh₂)OC(=CPh₂)] (156.4 (OCO), 150.7 (PCO), 125.9 (Ph₂C=COP), 95.5 (Ph₂C=CO₂ ppm) [97].

Pinacolate coupling was reported in the reaction of [NacNacAl] and benzophenone [98]. Magnesium complex [(dpp-bian)Mg(THF)₃] also reacts with benzophenone to create binuclear magnesium pinacolate [(dpp-bian)Mg(THF)₂{μ-O₂C₂Ph₄}], which can dissociate in toluene solution into two biradical species [99]. Analogously to these cases, generation of pinacolate **9** can be viewed through ketyl radical formation. Meanwhile, C–O coupling instead of C–C in the reaction of **1** with diphenylketene may account for the [1+2+2] cycloaddition mechanism. Besides transition metals [100] and phosphorus [97], ketene cyclization product **10** is the first to be reported across the main group metals.

A similar mechanism ambiguity between reduction and [1+2+2] cycloaddition appeared in the reaction of complex **1** with 2 equiv. of 1,2-dibenzylidenehydrazine. It resulted in complex [(dpp-bian)Ga{N(NCHPh)₂(CHPh)₂}[Na(DME)₃] (**11**) in the form of turquoise crystals at 39% yield. During the reaction, two benzaldazine molecules combined in the gallium atom coordination sphere. One C–C bond and two Ga–N bonds formed to create a five-membered galladiazametallacycle (Scheme 7).



Scheme 7. Reaction of **1** with 1,2-dibenzylidenehydrazine.

Compound **11** is diamagnetic and exhibits resolved NMR spectra. In the THF- d_8 solution, isopropyl substituents of the ligand appeared as a set of four doublets 6H and two septets 2H, indicative of a symmetry plane. The methine protons of benzaldazine are represented by two singlets at 7.37 and 5.08 ppm (2H each). The latter signal corresponds to the hydrogen atoms at the carbon atoms that formed a new bond. It shifted into the higher field compared to the starting 1,2-dibenzylidenehydrazine (cf. δ (NCHPh) $_2$ = 8.65 ppm). The naphthalene protons were not equivalent, which allowed us to conclude that the symmetry plane coincides with the naphthalene plane. The addition reaction was also nicely illustrated by ^{13}C NMR signals of 131.2 ppm (H–C=N) and 68.8 ppm (H–C–N) shifted in comparison to the starting material (cf. δ (–N=CPh) $_2$ = 161.8 ppm). The presence of the symmetry plane confirmed the formation of one optical isomer—the *meso*-form.

Curiously, when the DME solution of **1** was treated with 1 equiv. of 1,2-dibenzylidenehydrazine and then the products were dissolved in pyridine, a pyridine–benzaldazine coupling product [(dpp-bian)GaN(NCHPh)C(Ph)CN][Na(DME) $_3$] (**12**) was isolated in 40% yield as green crystals (Scheme 7). Using pyridine- d_5 as a solvent, an isostructural complex **12-d⁵** was isolated.

In the THF- d_8 solution, the molecule of **12** was asymmetric, which was seen from eight doublets and four septets arising from *i*Pr-substituents of dpp-bian (Figure 1). The methine protons of the azine fragment produced two distinct signals (1H each) at 7.73 and 4.58 ppm. The last corresponded to the hydrogen atom at the sp^3 -hybridized carbon atom, forming a new bond. Five signals of protons in the pyridine fragment (6.62, 5.44, 4.29, 4.23, 4.00 ppm) were significantly shifted in comparison to free pyridine (8.61, 7.66, 7.28 ppm), which confirmed its dearomatization. The assignment of these signals became clear when ^1H NMR spectra of **12** and **12-d⁵** were compared (Figure 1). The ^{13}C NMR spectrum also confirmed the structure of the resulting compound. The signal of the sp^3 -hybridized carbon atom H–C–N of the azine fragment shifted upfield (73.3 ppm), and the sp^2 -hybridized carbon atom H=C=N produced a signal at 131.5 ppm (cf. δ (–N=CPh) $_2$ 161.8 ppm). The carbon atoms of the pyridine fragment of **12** produced ^{13}C NMR signals at 143.7, 127.5, 104.6, 92.5, and 62.5 ppm. (cf. $\text{C}_5\text{H}_5\text{N}$ 149.9, 135.9, and 123.75 ppm in pyridine). Since only one diastereomer was identified in both reactions of **1** with benzaldazine, it may be believed to proceed through the cycloaddition mechanism.

Similar reductions of benzaldazine were reported by [(C_5Me_5) $_2\text{Sm}(\text{THF})_2$] [101] and [$\text{Cp}_2\text{Ti}(\eta^2\text{-Me}_3\text{SiC}_2\text{SiMe}_3)$] [102]. The authors suggested a one-electron reduction of the imino group, which led to C–C coupling binuclear complexes. Processes of chemoselective coupling of carbonyl compounds with pyridine were previously reported for [NacNacAl:] (NacNac = [ArNC-(Me)CHC(Me)NAr] $^-$, Ar = 2,6-*i*Pr $_2\text{C}_6\text{H}_3$) [81]. However, the coupling of two azine molecules and one azine molecule with a pyridine molecule in the coordination sphere of one metal atom was observed for the first time.

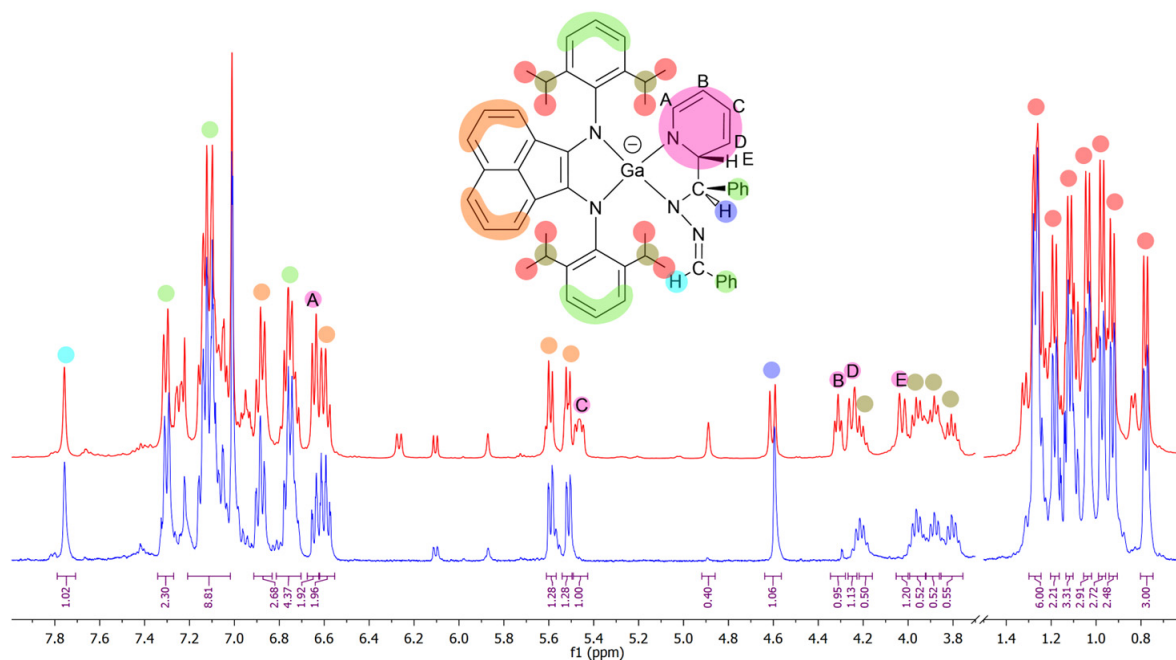


Figure 1. Selected area of ^1H NMR spectrum of **12** (red) and **12-d⁵** (blue) (THF-d^8 , 400 MHz, 25 °C).

Molecular Structures of Compounds 2–12

According to XRD analysis of **2–12**, interatomic bond distances within five-membered metallacycles correspond to single C–N and double C=C bonds and agree well with the geometry of complex **1** [103]. This anticipates that dpp-bian preserved the dianion state during the reactions, while electron transfer occurred exclusively from the metal atom.

The XRD analysis of **2** (Figure 2) indicated that radial interatomic distances N(3)–C(37) (1.277(2) Å) and N(5)–C(50) (1.284(2) Å) are close to the double C=N bonds (1.29 Å) distances, while N(4)–C(37) (1.414(2) Å), N(4)–C(50) (1.412(2) Å) are close to single C–N (1.47 Å). These values correlate well with distances in platinum complexes [(RCN)₂PtC(=NR)NRC(=NR)] (av. C=N 1.42, C–N 1.28 Å) [92] and the organic molecule imidoformamide (av. C=N 1.268, C–N 1.375 Å) [104].

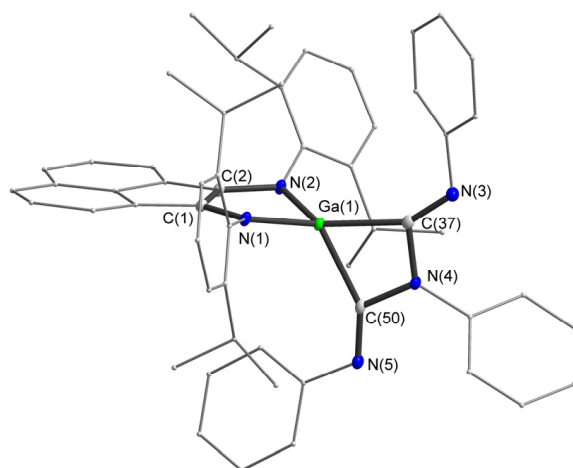


Figure 2. Molecular structure of anion **2**. Thermal ellipsoids are drawn at 30% probability level. Hydrogen atoms are omitted for clarity. Selected bond lengths (Å) and angles (°): N(1)–C(1) 1.380(2), N(2)–C(2) 1.401(2), C(1)–C(2) 1.379(2), N(3)–C(37) 1.277(2), N(4)–C(37) 1.414(2), N(4)–C(50) 1.412(2), N(5)–C(50) 1.284(2), Ga(1)–C(37) 2.0621(16), Ga(1)–C(50) 2.0635(16), N(3)–C(37)–N(4) 119.12(14), C(50)–N(4)–C(37) 109.86(13), N(5)–C(50)–N(4) 119.23(14) C(37)–Ga(1)–C(50) 68.20(6).

In the crystal, molecules of **3** presented by species dimerized through sodium cations and placed on the crystallographic center of symmetry (Figure 3). Distances O(1)–C(43) (1.2397(18) Å), O(2)–C(50) (1.2448(18) Å) are close to each other and correspond to a double C=O bond. The C–N bonds (N(3)–C(43) (1.3352(19) Å), N(5)–C(50) (1.3436(19) Å) are averaged between C=N (1.27 Å) and C–N (1.46 Å), probably due to conjugation with C=O bonds. Interatomic distances N(4)–C(50) (1.4174(19) Å) and N(4)–C(43) (1.4300(19) Å) in turn fall into the range typical to single C–N bonds. Interatomic distances corroborate those of N,N',N''-triphenylbiuret [105]. Complex **4**, like **3**, is a dimer in a crystal state (Figure 4). Interatomic distance O(2)–C(37) (1.239(6) Å) corresponds to a double C=O bond, while the distances O(1)–C(37) (1.345(6) Å) and N(3)–C(37) (1.366(6) Å) correspond to single C–O and C–N bonds. Similar four-member metallacycles MNCO were previously reported on aluminum [75]. Admittedly, structures **3** and **4** are reminiscent of reaction products of **1** with 1 equiv. of CO₂ and 1 equiv. of PhNCO or CyNCO [(dpp-bian)GaN(Cy)C(O)N(Cy)C(O)O]₂[Na(DME)₂]₂ and [(dpp-bian)GaN(Ph)C(O)O]₂[Na(DME)₂]₂, respectively [87].

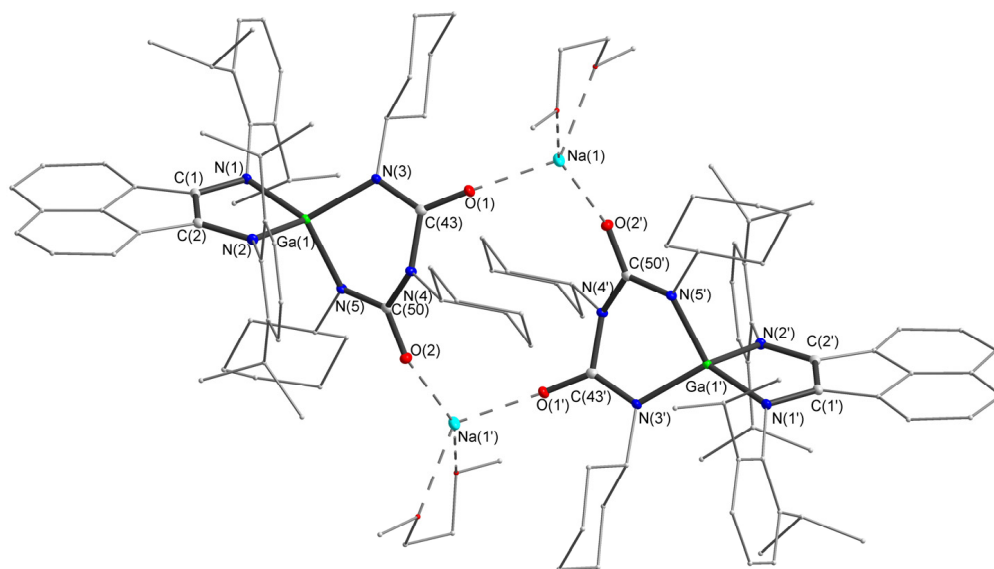


Figure 3. Molecular structure of compound **3**. Thermal ellipsoids are drawn at 30% probability level. Hydrogen atoms are omitted. Selected bond lengths (Å) and angles (°): Ga(1)–N(3) 1.9029(12), Ga(1)–N(5) 1.9301(13), O(1)–C(43) 1.2397(18), O(2)–C(50) 1.2448(18), N(4)–C(50) 1.4174(19), N(4)–C(43) 1.4300(19), N(5)–C(50) 1.3436(19), N(3)–C(43) 1.3352(19), N(3)–Ga(1)–N(5) 95.76(5), C(43)–N(3)–Ga(1) 117.45(10), N(3)–C(43)–N(4) 116.44(13), C(50)–N(4)–C(43) 124.69(12), C(50)–N(5)–Ga(1) 114.47(10), N(5)–C(50)–N(4) 117.95(13).

Metallacycle GaOCNC is not planar; the gallium atom is positioned out of a plane at 0.127 Å (Figure 5). Interatomic distances O(1)–C(37) (1.305(2) Å), N(3)–C(37) (1.383(3) Å), N(3)–C(44) (1.415(3) Å) are single C–O and C–N bonds, but O(2)–C(37) (1.228(2) Å) and N(4)–C(44) (1.265(3) Å) are shorter and correspond to double bonds. The structure of the organic fragment in **5** is parallel to the product of the insertion of carbodiimide into a carbamate, propane-2-yl (diphenylcarbamiidoyl)(phenyl)carbamate PhNHC(=NPh)NPhC(=O)OiPr, that was isolated from the reaction of titanium isopropoxide with phenylisocyanate [106].

According to XRD analysis, molecular structure of **6** (Figure S1) contains almost square fragment Ga₂O₂ with inner angles about 90° and close interatomic distances Ga–O (Ga(1)–O(1) 1.8322(16) Å, Ga(1)–O(1a) 1.8830(17) Å). Plane Ga₂O₂ is orthogonal to the plane of dpp-bian moiety (89.9°). This feature is reminiscent of other gallium oxo-complexes [107]. The Ga–Ga interatomic distance (2.6336(5) Å) is significantly less than the doubled value van der Waals radius (3.74 Å) [108]. However, given the significant ionic nature of gallium atoms, the Ga–Ga interactions are likely small.

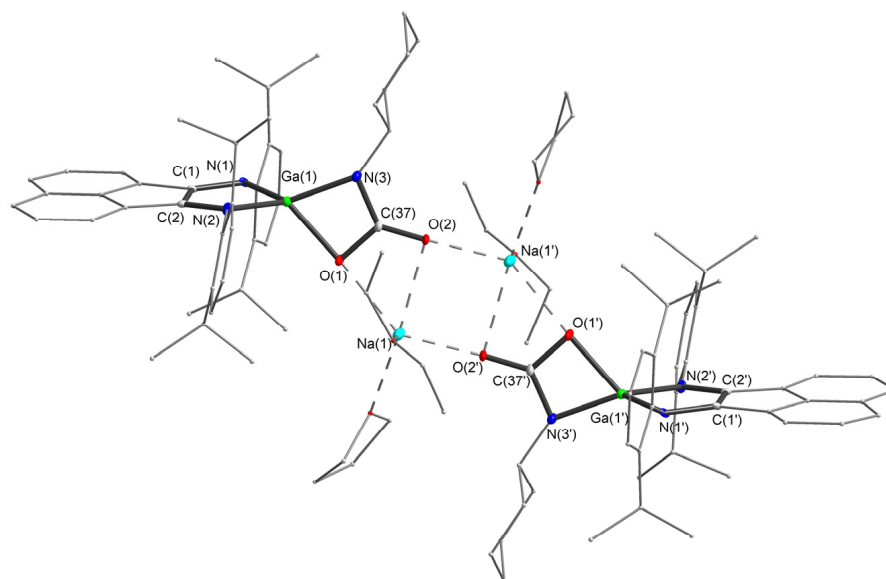


Figure 4. Molecular structure of compound **4**. Thermal ellipsoids are drawn at 30% probability level. Hydrogen atoms are omitted for clarity. Selected bond lengths (Å) and angles (°): Ga(1)–N(2) 1.882(5), Ga(1)–N(1) 1.889(5), Ga(1)–N(3) 1.902(4), Ga(1)–O(1) 1.984(3), N(1)–C(1) 1.389(9), C(1)–C(2) 1.394(7), N(2)–C(2) 1.403(9), O(1)–C(37) 1.345(6), O(2)–C(37) 1.239(6), N(3)–C(37) 1.366(6), C(37)–N(3)–Ga(1) 92.6(3), N(3)–Ga(1)–O(1) 68.96(17), C(37)–O(1)–Ga(1) 89.8(3), O(1)–C(37)–N(3) 108.6(5), O(2)–C(37)–O(1) 122.4(5), O(2)–C(37)–N(3) 129.0(5).

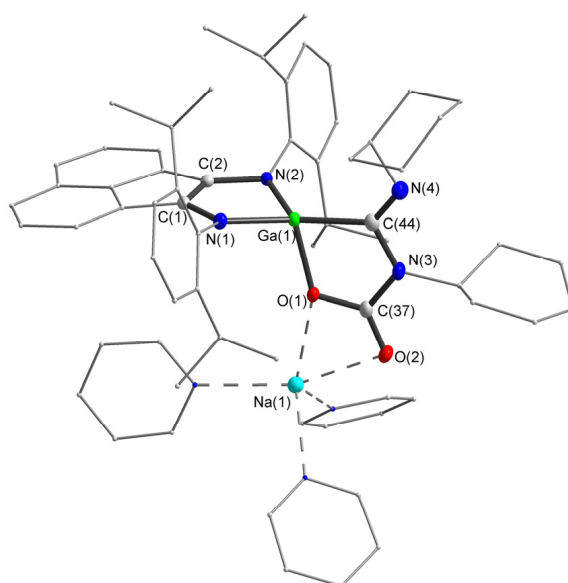


Figure 5. Molecular structure of compound **5**. Thermal ellipsoids are drawn at 30% probability level. Hydrogen atoms are omitted for clarity. Selected bond lengths (Å) and angles (°): N(1)–C(1) 1.394(2), N(2)–C(2) 1.391(2), C(1)–C(2) 1.368(3), N(3)–C(37) 1.383(3), O(1)–C(37) 1.305(2), O(2)–C(37) 1.228(2), N(3)–C(44) 1.415(3), N(4)–C(44) 1.265(3), Ga(1)–N(1) 1.8874(15), Ga(1)–N(2) 1.8908(15), Ga(1)–O(1) 1.9520(13), Ga(1)–C(44) 1.979(2), N(1)–Ga(1)–N(2) 90.29(7), N(1)–Ga(1)–O(1) 105.07(6), N(2)–Ga(1)–O(1) 109.23(6), N(1)–Ga(1)–C(44) 129.61(7), N(2)–Ga(1)–C(44) 134.14(8), O(1)–Ga(1)–C(44) 84.00(7), O(2)–C(37)–O(1) 121.95(19), O(2)–C(37)–N(3) 121.76(17), O(1)–C(37)–N(3) 116.29(17), N(4)–C(44)–N(3) 118.76(18), N(4)–C(44)–Ga(1) 133.90(16), N(3)–C(44)–Ga(1) 107.34(13).

Crystals of **8** suitable for XRD analysis were obtained by recrystallization from C_6D_6 (Figure 6). Bonds lengths in carbamate fragment O(2)–C(73) (1.2744(19) Å), O(3)–C(73) (1.2759(19) Å) are approximately equal and in good agreement with phenanthroline–

carboxylate gallium complex (C(30)–O(5) (1.269(12) Å) and C(30)–O(6) (1.272(11) Å)) [109]. The gallium oxide bridge geometry is similar that of **6**. The sum of the angles at the C(73) is approximately 360°, which indicates its sp²-hybridization.

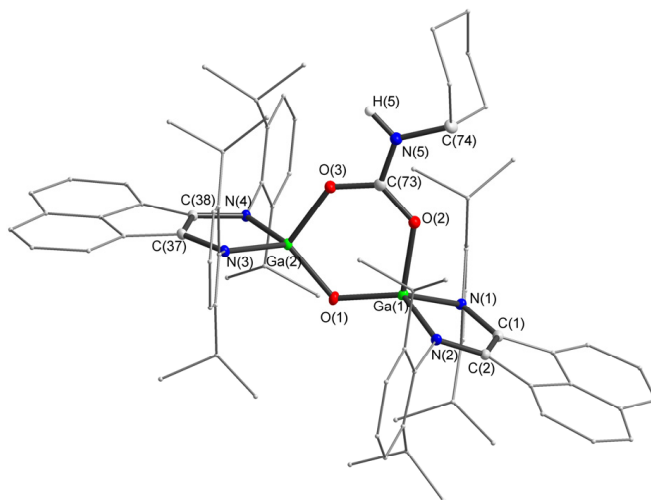


Figure 6. Molecular structure of anion **8**. Thermal ellipsoids are drawn at 30% probability level. Hydrogen atoms (except H(5)) are omitted. Selected bond lengths (Å) and angles (°): Ga(1)–N(1) 1.9047(12), Ga(1)–N(2) 1.9046(12), O(2)–C(73) 1.2743(19), O(3)–C(73) 1.2759(18), N(1)–C(1) 1.3929(19), N(2)–C(2) 1.3920(19), N(5)–C(73) 1.342(2), O(1)–Ga(1)–N(1) 124.00(5), O(1)–Ga(1)–O(2) 106.72(5), Ga(1)–O(1)–Ga(2) 123.34(7), O(2)–C(73)–O(3) 125.90(14), O(2)–C(73)–N(5) 118.38(14), O(3)–C(73)–N(5) 115.73(14).

The molecular structure of products **9** and **10** is shown in Figure 7. They consist of galladioxolene metallacycles. Bonds within the metallacycles (O(1)–C(37) 1.4184(15), O(2)–C(50) 1.4377(15), C(37)–C(50) 1.6408(18), Ga(1)–O(1) 1.8310(9), Ga(1)–O(2) 1.8654(9) Å in **9** and O(43)–C(44) 1.313(6), O(45)–C(44) 1.370(6), O(45)–C(46) 1.408(6), Ga(1)–O(43) 1.921(4), Ga(1)–C(46) 1.978(5) Å in **10**) are in perfect agreement with expected values (C–C 1.52, C–O 1.42, C(sp²)–O 1.39, Ga–O 1.88, Ga–C(sp²) 1.95 Å) derived from corresponding covalent radii [110]. Compared to **9**, the metallacycle in **10** is almost flat; the deviation of atoms from this plane is less than 0.033 Å. The sum of the angles at the carbon atoms C(44) and C(46) in **10** is approximately 360°, indicating their sp²-hybridization. Bond lengths C(44)–C(66) (1.372(8) Å) and C(46)–C(47) (1.333(8) Å) correspond to double C=C bonds (1.34 Å). Pinacolates fragments can be compared with similar complexes, for example, aluminum pinacolates [Al(OCPh₂)₂] (L = HC[(CMe)(NAr)]₂, Ar = 2,6-*i*-Pr₂C₆H₃) [98]. Comparison of metallacycle in **10** is limited to germanium cycloadduct [LGeC(Ph)OC(Ph)O] (O(1)–C(21) 1.416(2) Å, O(2)–C(21) 1.433(2) Å, O(2)–C(28) 1.435(2) Å) [111], and the titanium complex [(Cp)₂TiC(=CPh₂)OC(=CPh₂)O] (O(1)–C(11) 1.36(2) Å, O(2)–C(11) 1.33(2) Å, O(2)–C(13) 1.42(2) Å) [100].

The compounds **11** and **12** were characterized by XRD (Figure 8). During the reaction, the double C=N bond is reduced to a single one, as can be clearly seen from a comparison of C(38)–N(5) (1.4578(16) Å) and N(6)–C(58) (1.2903(18) Å) interatomic distances in **11**. Bonds N(5)–N(6) (1.3584(15) Å) and N(3)–N(4) (1.3547(16) Å) are also elongated by 0.6 Å in comparison to free benzaldazine (1.418 Å) [112] due to loss of conjugation. These changes are consistent with the geometry of the reduced benzaldazine fragment in [Cp₂Ti(η²-Me₃SiC₂SiMe₃)] [102]. The same considerations are true for the benzaldazine fragment of **12**. On top of that, the pyridine molecule in **12** loses its aromaticity, which is clear from a comparison of the interatomic distances of a pyridine fragment, where N(5)–C(41) (1.428(8) Å), N(5)–C(37) (1.363(8) Å) are single C–N bonds, C(38)–C(39) (1.443(10) Å) are C–C bonds, and C(37)–C(38) (1.347(7) Å), C(40)–C(39) (1.383(10) Å) are double C=C bonds. Compound **12** is chiral due to the two asymmetric centers, C(41) and C(42), with an *S*-

configuration. Compound **12** crystallizes in the centrosymmetric group $P2_1/C$, so the enantiomer is also present in the crystal.

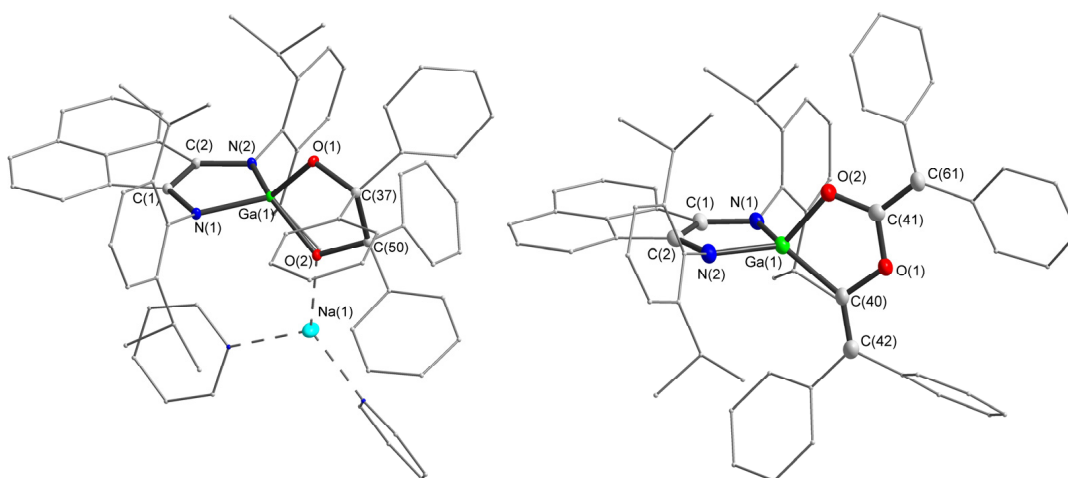


Figure 7. Molecular structures of compound **9** and anion of **10**. Thermal ellipsoids are drawn at 30% probability level. Hydrogen atoms are omitted for clarity. Selected bond lengths (Å) and angles (°) in **9**: N(1)–C(1) 1.3988(16), C(1)–C(2) 1.3799(18), N(2)–C(2) 1.3901(16), Ga(1)–O(1) 1.8310(9), Ga(1)–O(2) 1.8654(9), O(1)–C(37) 1.4184(15), O(2)–C(50) 1.4377(15), C(37)–C(50) 1.6408(18), O(1)–Ga(1)–O(2) 89.30(4), O(1)–C(37)–C(50) 107.94(10), C(37)–O(1)–Ga(1) 114.14(8), C(50)–O(2)–Ga(1) 112.25(7), O(2)–C(50)–C(37) 105.97(10), C(57)–C(50)–C(51) 113.06(11), C(38)–C(37)–C(44) 107.86(10). Selected bond lengths (Å) and angles (°) in **10**: N(2)–C(15) 1.392(7), C(16)–C(15) 1.385(7), N(17)–C(16) 1.375(7), Ga(1)–O(43) 1.921(4), Ga(1)–C(46) 1.978(5), O(43)–C(44) 1.313(6), O(45)–C(44) 1.370(6), O(45)–C(46) 1.408(6), C(44)–C(66) 1.372(8), C(46)–C(47) 1.333(8), O(43)–Ga(1)–C(46) 84.67(19), O(43)–C(44)–O(45) 117.1(5), O(43)–C(44)–C(66) 123.4(5), O(45)–C(44)–C(66) 119.5(5).

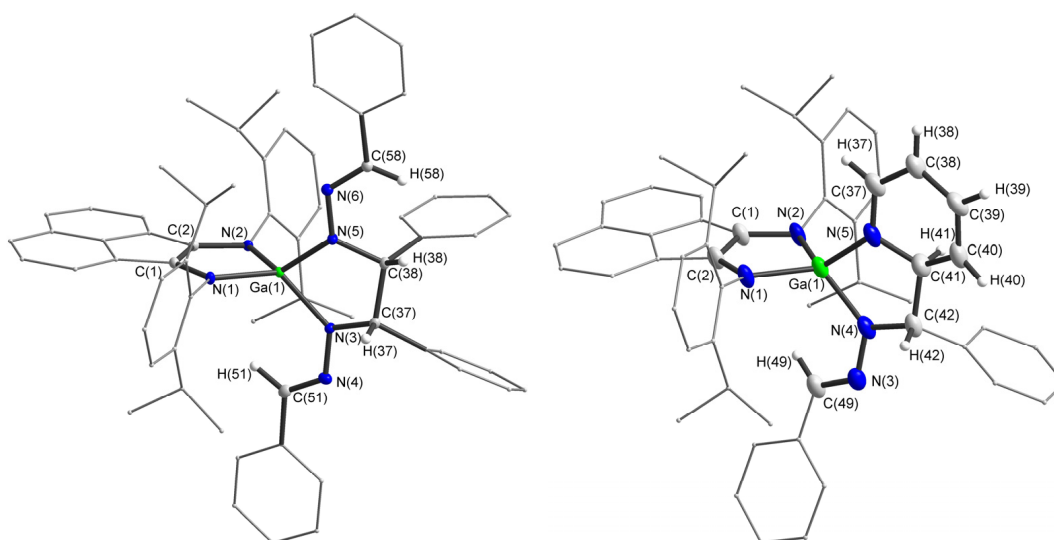


Figure 8. Molecular structures of anions **11** and **12**. Thermal ellipsoids are drawn at 30% probability level. Hydrogen atoms except for H(58), H(38), H(37), H(51) in **11** and H(37), H(38), H(39), H(40), H(41), H(42), H(49) in **12** are omitted. Selected bond lengths (Å) and angles (°) in **11**: N(1)–C(1) 1.3871(16), C(1)–C(2) 1.3805(18), N(2)–C(2) 1.3884(16), N(5)–N(6) 1.3584(15), N(5)–C(38) 1.4578(16), N(6)–C(58) 1.2903(18), C(37)–C(38) 1.5629(19), N(3)–C(37) 1.4637(17), N(3)–N(4) 1.3547(16), N(4)–C(51) 1.2721(19), N(4)–N(3)–C(37) 111.43(10), C(51)–N(4)–N(3) 119.86(12), N(6)–N(5)–C(38) 120.00(11), C(58)–N(6)–N(5) 120.79(11), N(3)–C(37)–C(38) 108.19(10), N(5)–C(38)–C(37) 106.35(10), N(4)–C(51)–C(52) 120.14(13), N(6)–C(58)–C(59) 121.14(13). Selected bond lengths (Å) and angles (°) in **12**: Ga(1)–N(5)

1.897(4), Ga(1)–N(4) 1.890(6), Ga(1)–N(1) 1.926(4), Ga(1)–N(2) 1.886(4), N(5)–C(41) 1.428(8), C(42)–C(41) 1.550(9), N(4)–C(42) 1.476(6), N(3)–C(49) 1.290(7), N(4)–N(3) 1.375(7), N(1)–C(1) 1.375(7), C(1)–C(2) 1.369(7), N(2)–C(2) 1.409(7), N(4)–Ga(1)–N(5) 87.9(2), N(2)–Ga(1)–N(1) 89.79(18), N(4)–C(42)–C(41) 106.5(5), N(5)–C(41)–C(42) 113.3(5), N(5)–C(41)–C(40) 116.7(6), C(41)–N(5)–Ga(1) 111.2(4), C(42)–N(4)–Ga(1) 113.9(4), C(49)–N(3)–N(4) 116.3(5).

4. Conclusions

In conclusion, transformations of isocyanates, nitrous oxide, carbonyl sulfide, benzophenone, diphenylketene, benzaldazine, and pyridine at the Ga^I center combined with redox-active ligand dpp-bian were reported. They primarily resulted in cycloaddition products that reflected the gallium center's transition metal-like properties. The reactions were always aggravated by strong reductive behavior of low-valent centers, and a complete oxygen atom or other group transfer was sometimes observed. Simultaneously, the gallium center exhibited an exciting balance between the strong oxo- and carbophilicity, giving rise to products like imidoformamide **2**. This manuscript, together with papers concerning transformations of RN=C=NR [86] and O=C=O [87] substrates, illustrates that the Ga(I)-center supported with bisamide ligand can promote coupling of several C=O- and C=N- substrates to give plentiful organic products. One of the most notable features was coupling benzaldazine molecules with a robust substrate such as pyridine. That may open up more sustainable and selective alternatives for syntheses of imidoformamide, biuret, carbamic acid compounds, as well as opportunities to use gallylene reagents in McMurry- and Wittig-type reactions, selective C–C reductive couplings, and cyclizations.

Supplementary Materials: The following supporting information can be downloaded at: <https://www.mdpi.com/article/10.3390/reactions5010009/s1>, Details of synthesis, characterization, X-ray crystal structure determination details, and crystal data are given in the electronic supporting information. Figure S1: Molecular structure of compound **6**; Figure S2: Molecular structure of compound **7**; Figures S2–S46: NMR spectra of compounds **2**, **5**, **6**, **8–12**. Table S1. Crystallographic data and refinement details for compounds **2–12**. References [88,113–123] are cited in the Supplementary Materials.

Author Contributions: Conceptualization, I.L.F.; Methodology, O.A.K.; Validation, O.A.K. and E.V.B.; Formal analysis, O.A.K. and E.V.B.; Investigation, V.A.D.; Writing—original draft, V.A.D. and O.A.K.; Writing—review & editing, V.A.D., O.A.K., E.V.B. and I.L.F.; Supervision, I.L.F.; Project administration, V.A.D.; Funding acquisition, V.A.D. All authors have read and agreed to the published version of the manuscript.

Funding: This research was funded by the Russian Science Foundation, grant number 21-73-20153.

Data Availability Statement: The data that support the findings of this study are available from the corresponding authors upon reasonable request.

Acknowledgments: The authors thank the Analytical Center of the G.A. Razuvaev Institute of Organometallic Chemistry.

Conflicts of Interest: The authors declare no conflicts of interest.

References

1. Hopkinson, M.N.; Richter, C.; Schedler, M.; Glorius, F. An overview of N-heterocyclic carbenes. *Nature* **2014**, *510*, 485–496. [[CrossRef](#)]
2. Scholl, M.; Trnka, T.M.; Morgan, J.P.; Grubbs, R.H. Increased ring closing metathesis activity of ruthenium-based olefin metathesis catalysts coordinated with imidazolin-2-ylidene ligands. *Tetrahedron Lett.* **1999**, *40*, 2247–2250. [[CrossRef](#)]
3. Soleilhavoup, M.; Bertrand, G. Cyclic (Alkyl)(Amino)Carbenes (CAACs): Stable Carbenes on the Rise. *Acc. Chem. Res.* **2015**, *48*, 256–266. [[CrossRef](#)] [[PubMed](#)]
4. Bourissou, D.; Guerret, O.; Gabbai, F.P.; Bertrand, G. Stable Carbenes. *Chem. Rev.* **2000**, *100*, 39–92. [[CrossRef](#)] [[PubMed](#)]
5. Nesterov, V.; Reiter, D.; Bag, P.; Frisch, P.; Holzner, R.; Porzelt, A.; Inoue, S. NHCs in Main Group Chemistry. *Chem. Rev.* **2018**, *118*, 9678–9842. [[CrossRef](#)]
6. Moerdyk, J.P.; Bielawski, C.W. Reductive generation of stable, five-membered N,N'-diamidocarbenes. *Chem. Commun.* **2014**, *50*, 4551–4553. [[CrossRef](#)]

7. Dohmeier, C.; Robl, C.; Tacke, M.; Schnöckel, H. The Tetrameric Aluminum(I) Compound $[\{\text{Al}(\eta^5\text{-C}_5\text{Me}_5)\}_4]$. *Angew. Chem. Int. Ed.* **1991**, *30*, 564–565. [[CrossRef](#)]
8. Uhl, W.; Hiller, W.; Layh, M.; Schwarz, W. $[\text{Ga}_4\{\text{C}(\text{SiMe}_3)_3\}_4]$ with a Tetrahedral Ga_4 Skeleton. *Angew. Chem. Int. Ed.* **1992**, *31*, 1364–1366. [[CrossRef](#)]
9. Su, J.; Li, X.-W.; Crittendon, R.C.; Robinson, G.H. How Short is a -Ga-Ga- Triple Bond? Synthesis and Molecular Structure of $\text{Na}_2[\text{Mes}^*_2\text{C}_6\text{H}_3\text{-Ga-Ga-C}_6\text{H}_3\text{Mes}^*_2]$ ($\text{Mes}^* = 2,4,6\text{-i-Pr}_3\text{C}_6\text{H}_2$): The First Gallyne. *J. Am. Chem. Soc.* **1997**, *119*, 5471–5472. [[CrossRef](#)]
10. Wright, R.J.; Brynda, M.; Power, P.P. Synthesis and Structure of the “Dialuminyne” $\text{Na}_2[\text{Ar}'\text{AlAlAr}']$ and $\text{Na}_2[(\text{Ar}''\text{Al})_3]$: Al-Al Bonding in Al_2Na_2 and Al_3Na_2 Clusters. *Angew. Chem. Int. Ed.* **2006**, *45*, 5953–5956. [[CrossRef](#)]
11. Bag, P.; Porzelt, A.; Altmann, P.J.; Inoue, S. A Stable Neutral Compound with an Aluminum–Aluminum Double Bond. *J. Am. Chem. Soc.* **2017**, *139*, 14384–14387. [[CrossRef](#)]
12. Queen, J.D.; Lehmann, A.; Fettingner, J.C.; Tuononen, H.M.; Power, P.P. The Monomeric Alane-diyl: AlAr^iPr^8 ($\text{AriPr}^8 = \text{C}_6\text{H-2,6-(C}_6\text{H}_2\text{-2,4,6-Pri}_3)_2\text{-3,5-Pri}_2$): An Organoaluminum(I) Compound with a One-Coordinate Aluminum Atom. *J. Am. Chem. Soc.* **2020**, *142*, 20554–20559. [[CrossRef](#)]
13. Hicks, J.; Vasko, P.; Goicoechea, J.M.; Aldridge, S. Synthesis, structure and reaction chemistry of a nucleophilic aluminyl anion. *Nature* **2018**, *557*, 92–95. [[CrossRef](#)] [[PubMed](#)]
14. Schwamm, R.J.; Anker, M.D.; Lein, M.; Coles, M.P. Reduction vs. Addition: The Reaction of an Aluminyl Anion with 1,3,5,7-Cyclooctatetraene. *Angew. Chem. Int. Ed.* **2019**, *58*, 1489–1493. [[CrossRef](#)] [[PubMed](#)]
15. Grams, S.; Eysel, J.; Langer, J.; Färber, C.; Harder, S. Boosting Low-Valent Aluminum(I) Reactivity with a Potassium Reagent. *Angew. Chem. Int. Ed.* **2020**, *59*, 15982–15986. [[CrossRef](#)] [[PubMed](#)]
16. Kurumada, S.; Takamori, S.; Yamashita, M. An alkyl-substituted aluminium anion with strong basicity and nucleophilicity. *Nat. Chem.* **2020**, *12*, 36–39. [[CrossRef](#)]
17. Schmidt, E.S.; Jockisch, A.; Schmidbaur, H. A Carbene Analogue with Low-Valent Gallium as a Heteroatom in a quasi-Aromatic Imidazolate Anion. *J. Am. Chem. Soc.* **1999**, *121*, 9758–9759. [[CrossRef](#)]
18. Asay, M.; Jones, C.; Driess, M. N-Heterocyclic Carbene Analogues with Low-Valent Group 13 and Group 14 Elements: Syntheses, Structures, and Reactivities of a New Generation of Multitalented Ligands. *Chem. Rev.* **2011**, *111*, 354–396. [[CrossRef](#)]
19. Abdalla, J.A.B.; Aldridge, S. Group 13 Metal–Metal Bonds. In *Molecular Metal-Metal Bonds*; Wiley: Hoboken, NJ, USA, 2015; pp. 455–484.
20. Liu, Y.; Li, S.; Yang, X.-J.; Li, Q.-S.; Xie, Y.; Schaefer, H.F.; Wu, B. Alkali metal compounds of a gallium(I) carbene analogue $\{\text{Ga}[\text{N}(\text{Ar})\text{C}(\text{Me})_2]\}$ ($\text{Ar} = 2,6\text{-i-Pr}_2\text{C}_6\text{H}_3$). *J. Organomet. Chem.* **2011**, *696*, 1450–1455. [[CrossRef](#)]
21. Zhao, Y.; Liu, Y.; Li, Q.-S.; Su, J.-H. Synthesis and structures of mononuclear and dinuclear gallium complexes with α -diimine ligands: Reduction of the metal or ligand? *Dalton Trans.* **2016**, *45*, 246–252. [[CrossRef](#)]
22. Chen, W.; Zhao, Y.; Xu, W.; Su, J.-H.; Shen, L.; Liu, L.; Wu, B.; Yang, X.-J. Reductive linear- and cyclo-trimerization of isocyanides using an Al–Al-bonded compound. *Chem. Commun.* **2019**, *55*, 9452–9455. [[CrossRef](#)]
23. Koshino, K.; Kinjo, R. Construction of σ -Aromatic AlB_2 Ring via Borane Coupling with a Dicoordinate Cyclic (Alkyl)(Amino)Aluminyl Anion. *J. Am. Chem. Soc.* **2020**, *142*, 9057–9062. [[CrossRef](#)]
24. Yan, C.; Kinjo, R. A Three-Membered Diazo-Aluminum Heterocycle to Access an $\text{Al}=\text{C}$ π Bonding Species. *Angew. Chem. Int. Ed.* **2022**, *61*, e202211800. [[CrossRef](#)]
25. Fedushkin, I.L.; Skatova, A.A.; Dodonov, V.A.; Chudakova, V.A.; Bazyakina, N.L.; Piskunov, A.V.; Demeshko, S.V.; Fukin, G.K. Digallane with Redox-Active Diimine Ligand: Dualism of Electron-Transfer Reactions. *Inorg. Chem.* **2014**, *53*, 5159–5170. [[CrossRef](#)] [[PubMed](#)]
26. Dodonov, V.A.; Makarov, V.M.; Zemnyukova, M.N.; Razborov, D.A.; Baranov, E.V.; Bogomyakov, A.S.; Ovcharenko, V.I.; Fedushkin, I.L. Stability and Solution Behavior of $[(\text{dpp-Bian})\text{Ln}]$ and $[(\text{dpp-Bian})\text{LnX}]$ ($\text{Ln} = \text{Yb, Tm, or Dy}$; $\text{X} = \text{I, F, or N}_3$). *Organometallics* **2023**, *42*, 2558–2567. [[CrossRef](#)]
27. Dodonov, V.A.; Chen, W.; Zhao, Y.; Skatova, A.A.; Roesky, P.W.; Wu, B.; Yang, X.J.; Fedushkin, I.L. Gallium “Shears” for C=N and C=O Bonds of Isocyanates. *Chem. Eur. J.* **2019**, *25*, 8259–8267. [[CrossRef](#)] [[PubMed](#)]
28. Dodonov, V.A.; Chen, W.; Liu, L.; Sokolov, V.G.; Baranov, E.V.; Skatova, A.A.; Zhao, Y.; Wu, B.; Yang, X.-J.; Fedushkin, I.L. Reactions of Iso(thio)cyanates with Dialanes: Cycloaddition, Reductive Coupling, or Cleavage of the C=S or C=O Bond. *Inorg. Chem.* **2021**, *60*, 14602–14612. [[CrossRef](#)] [[PubMed](#)]
29. Fedushkin, I.L.; Skatova, A.A.; Dodonov, V.A.; Yang, X.-J.; Chudakova, V.A.; Piskunov, A.V.; Demeshko, S.; Baranov, E.V. Ligand “Brackets” for Ga–Ga Bond. *Inorg. Chem.* **2016**, *55*, 9047–9056. [[CrossRef](#)] [[PubMed](#)]
30. Zhang, Y.; Dodonov, V.A.; Chen, W.; Zhang, S.; Roesky, P.W.; Zhao, Y.; Fedushkin, I.L.; Yang, X.-J. Reactions of Low-Valent Gallium Species with Organic Azides: Formation of Imido-, Azoimido-, and Tetrazene Complexes. *Inorg. Chem.* **2023**, *62*, 6288–6296. [[CrossRef](#)]
31. Fedushkin, I.L.; Dodonov, V.A.; Skatova, A.A.; Sokolov, V.G.; Piskunov, A.V.; Fukin, G.K. Redox-Active Ligand-Assisted Two-Electron Oxidative Addition to Gallium(II). *Chem. Eur. J.* **2018**, *24*, 1877–1889. [[CrossRef](#)]
32. Dodonov, V.A.; Morozov, A.G.; Romyantsev, R.V.; Fukin, G.K.; Skatova, A.A.; Roesky, P.W.; Fedushkin, I.L. Synthesis and ϵ -Caprolactone Polymerization Activity of Electron-Deficient Gallium and Aluminum Species Containing a Charged Redox-Active dpp-Bian Ligand. *Inorg. Chem.* **2019**, *58*, 16559–16573. [[CrossRef](#)] [[PubMed](#)]

33. Zhong, M.; Sinhababu, S.; Roesky, H.W. The unique β -diketiminate ligand in aluminum(I) and gallium(I) chemistry. *Dalton Trans.* **2020**, *49*, 1351–1364. [[CrossRef](#)]
34. Nagendran, S.; Roesky, H.W. The Chemistry of Aluminum(I), Silicon(II), and Germanium(II). *Organometallics* **2008**, *27*, 457–492. [[CrossRef](#)]
35. Lopez, C.A. Aluminium, gallium, indium and thallium. *Annu. Rep. Sect. A* **2009**, *105*, 98–116. [[CrossRef](#)]
36. Schoeller, W.W. Neutral Carbene Analogues of Group 13 Elements: The Dimerization Reaction to a Biradicaloid. *Inorg. Chem.* **2011**, *50*, 2629–2633. [[CrossRef](#)] [[PubMed](#)]
37. Bai, Y.; Chen, W.; Li, J.; Cui, C. Chemistry of s-, p- and f-block metal complexes with ene-diamido ligands. *Coord. Chem. Rev.* **2019**, *383*, 132–154. [[CrossRef](#)]
38. Helling, C.; Schulz, S. Thallium. In *Comprehensive Organometallic Chemistry IV*; Parkin, G., Meyer, K., O'hare, D., Eds.; Elsevier: Oxford, UK, 2022; pp. 370–406.
39. Linti, G.; Schnöckel, H. Low valent aluminum and gallium compounds—Structural variety and coordination modes to transition metal fragments. *Coord. Chem. Rev.* **2000**, *206–207*, 285–319. [[CrossRef](#)]
40. González-Gallardo, S.; Bollermann, T.; Fischer, R.A.; Murugavel, R. Cyclopentadiene Based Low-Valent Group 13 Metal Compounds: Ligands in Coordination Chemistry and Link between Metal Rich Molecules and Intermetallic Materials. *Chem. Rev.* **2012**, *112*, 3136–3170. [[CrossRef](#)]
41. Zhang, X.; Liu, L.L. Modulating the Frontier Orbitals of an Aluminylene for Facile Dearomatization of Inert Arenes. *Angew. Chem. Int. Ed.* **2022**, *61*, e202116658. [[CrossRef](#)]
42. Dhara, D.; Jayaraman, A.; Härterich, M.; Dewhurst, R.D.; Braunschweig, H. Generation of a transient base-stabilised arylaluminum for the facile deconstruction of aromatic molecules. *Chem. Sci.* **2022**, *13*, 5631–5638. [[CrossRef](#)]
43. Dmitrienko, A.; Pilkington, M.; Britten, J.F.; Gabidullin, B.M.; van der Est, A.; Nikonov, G.I. Shedding Light on the Diverse Reactivity of NaCNAl with N-Heterocycles. *Angew. Chem. Int. Ed.* **2020**, *59*, 16147–16153. [[CrossRef](#)] [[PubMed](#)]
44. Kassymbek, A.; Vyboishchikov, S.F.; Gabidullin, B.M.; Spasyuk, D.; Pilkington, M.; Nikonov, G.I. Sequential Oxidation and C–H Bond Activation at a Gallium(I) Center. *Angew. Chem. Int. Ed.* **2019**, *58*, 18102–18107. [[CrossRef](#)] [[PubMed](#)]
45. Kassymbek, A.; Spasyuk, D.; Dmitrienko, A.; Pilkington, M.; Nikonov, G.I. Facile C–H bond activation on a transient gallium imide. *Chem. Commun.* **2022**, *58*, 6946–6949. [[CrossRef](#)] [[PubMed](#)]
46. Chu, T.; Boyko, Y.; Korobkov, I.; Nikonov, G.I. Transition Metal-like Oxidative Addition of C–F and C–O Bonds to an Aluminum(I) Center. *Organometallics* **2015**, *34*, 5363–5365. [[CrossRef](#)]
47. Chu, T.; Vyboishchikov, S.F.; Gabidullin, B.M.; Nikonov, G.I. Oxidative Cleavage of the C=N Bond on Al(I). *J. Am. Chem. Soc.* **2017**, *139*, 8804–8807. [[CrossRef](#)] [[PubMed](#)]
48. Chu, T.; Vyboishchikov, S.F.; Gabidullin, B.; Nikonov, G.I. Oxidative Cleavage of C=S and P=S Bonds at an AlI Center: Preparation of Terminally Bound Aluminum Sulfides. *Angew. Chem. Int. Ed.* **2016**, *55*, 13306–13311. [[CrossRef](#)] [[PubMed](#)]
49. Seifert, A.; Scheid, D.; Linti, G.; Zessin, T. Oxidative Addition Reactions of Element–Hydrogen Bonds with Different Polarities to a Gallium(I) Compound. *Chem. Eur. J.* **2009**, *15*, 12114–12120. [[CrossRef](#)] [[PubMed](#)]
50. Chu, T.; Korobkov, I.; Nikonov, G.I. Oxidative Addition of σ Bonds to an Al(I) Center. *J. Am. Chem. Soc.* **2014**, *136*, 9195–9202. [[CrossRef](#)]
51. Chu, T.; Boyko, Y.; Korobkov, I.; Kuzmina, L.G.; Howard, J.A.K.; Nikonov, G.I. Oxidative Addition of Disulfides, Alkyl Sulfides, and Diphosphides to an Aluminum(I) Center. *Inorg. Chem.* **2016**, *55*, 9099–9104. [[CrossRef](#)]
52. Falconer, R.L.; Nichol, G.S.; Smolyar, I.V.; Cockroft, S.L.; Cowley, M.J. Reversible Reductive Elimination in Aluminum(II) Dihydrides. *Angew. Chem. Int. Ed.* **2021**, *60*, 2047–2052. [[CrossRef](#)]
53. Chu, T.; Nikonov, G.I. Oxidative Addition and Reductive Elimination at Main-Group Element Centers. *Chem. Rev.* **2018**, *118*, 3608–3680. [[CrossRef](#)]
54. Weetman, C.; Inoue, S. The Road Travelled: After Main-Group Elements as Transition Metals. *ChemCatChem* **2018**, *10*, 4213–4228. [[CrossRef](#)]
55. Ota, K.; Kinjo, R. Heavier element-containing aromatics of $[4n + 2]$ -electron systems. *Chem. Soc. Rev.* **2021**, *50*, 10594–10673. [[CrossRef](#)] [[PubMed](#)]
56. Weetman, C.; Bag, P.; Szilvási, T.; Jandl, C.; Inoue, S. CO₂ Fixation and Catalytic Reduction by a Neutral Aluminum Double Bond. *Angew. Chem. Int. Ed.* **2019**, *58*, 10961–10965. [[CrossRef](#)] [[PubMed](#)]
57. Weetman, C.; Porzelt, A.; Bag, P.; Hanusch, F.; Inoue, S. Dialumenes—Aryl vs. silyl stabilisation for small molecule activation and catalysis. *Chem. Sci.* **2020**, *11*, 4817–4827. [[CrossRef](#)] [[PubMed](#)]
58. Cui, C.; Li, X.; Wang, C.; Zhang, J.; Cheng, J.; Zhu, X. Isolation of a 1,2-Dialuminacyclobutene. *Angew. Chem. Int. Ed.* **2006**, *45*, 2245–2247. [[CrossRef](#)] [[PubMed](#)]
59. Agou, T.; Nagata, K.; Tokitoh, N. Synthesis of a Dialumene-Benzene Adduct and Its Reactivity as a Synthetic Equivalent of a Dialumene. *Angew. Chem. Int. Ed.* **2013**, *52*, 10818–10821. [[CrossRef](#)] [[PubMed](#)]
60. Queen, J.D.; Power, P.P. Comproportionation of a dialuminyne with alane or dialane dihalides as a clean route to dialuminenes. *Chem. Commun.* **2023**, *59*, 43–46. [[CrossRef](#)] [[PubMed](#)]
61. Caputo, C.A.; Zhu, Z.; Brown, Z.D.; Fettingner, J.C.; Power, P.P. Activation of olefins with low-valent gallium compounds under ambient conditions. *Chem. Commun.* **2011**, *47*, 7506–7508. [[CrossRef](#)] [[PubMed](#)]

62. Zhu, H.; Chai, J.; Fan, H.; Roesky, H.W.; He, C.; Jancik, V.; Schmidt, H.-G.; Noltemeyer, M.; Merrill, W.A.; Power, P.P. A Stable Aluminacyclopentene $\text{LAl}(\eta^2\text{-C}_2\text{H}_2)$ and Its End-On Azide Insertion to an Aluminaazacyclobutene. *Angew. Chem. Int. Ed.* **2005**, *44*, 5090–5093. [[CrossRef](#)]
63. Bakewell, C.; White, A.J.P.; Crimmin, M.R. Reversible alkene binding and allylic C–H activation with an aluminium(I) complex. *Chem. Sci.* **2019**, *10*, 2452–2458. [[CrossRef](#)] [[PubMed](#)]
64. Bakewell, C.; Garçon, M.; Kong, R.Y.; O'Hare, L.; White, A.J.P.; Crimmin, M.R. Reactions of an Aluminum(I) Reagent with 1,2-, 1,3-, and 1,5-Dienes: Dearomatization, Reversibility, and a Pericyclic Mechanism. *Inorg. Chem.* **2020**, *59*, 4608–4616. [[CrossRef](#)] [[PubMed](#)]
65. Dmitrienko, A.; Pilkington, M.; Nikonov, G.I. Reactions of an aluminium(I) diketiminate compound with arenes. *Mendeleev Commun.* **2022**, *32*, 68–70. [[CrossRef](#)]
66. Dmitrienko, A.; Britten, J.F.; Spasyuk, D.; Nikonov, G.I. Adduct of NacNacAl with Benzophenone and Its Coupling Chemistry. *Chem. Eur. J.* **2020**, *26*, 206–211. [[CrossRef](#)]
67. Koner, A.; Gabidullin, B.M.; Kelemen, Z.; Nyulászi, L.; Nikonov, G.I.; Streubel, R. 7-Metalla-1,4-diphosphanorbornadienes: Cycloaddition of monovalent group 13 NacNac complexes to a stable 1,4-diphosphinine. *Dalton Trans.* **2019**, *48*, 8248–8253. [[CrossRef](#)] [[PubMed](#)]
68. Sugita, K.; Nakano, R.; Yamashita, M. Cycloaddition of Dialkylaluminum Anion toward Unsaturated Hydrocarbons in (1 + 2) and (1 + 4) Modes. *Chem. Eur. J.* **2020**, *26*, 2174–2177. [[CrossRef](#)]
69. Kassymbek, A.; Britten, J.F.; Spasyuk, D.; Gabidullin, B.; Nikonov, G.I. Interaction of Multiple Bonds with NacNacGa : Oxidative Cleavage vs. Coupling and Cyclization. *Inorg. Chem.* **2019**, *58*, 8665–8672. [[CrossRef](#)]
70. Loh, Y.K.; Aldridge, S. Acid–Base Free Main Group Carbonyl Analogues. *Angew. Chem. Int. Ed.* **2021**, *60*, 8626–8648. [[CrossRef](#)]
71. Fooker, U.; Saak, W.; Weidenbruch, M. Diarylstannylene reactions with some aryl azides: Formation of different ring systems. *J. Organomet. Chem.* **1999**, *579*, 280–284. [[CrossRef](#)]
72. Anker, M.D.; Coles, M.P. Aluminium-Mediated Carbon Dioxide Reduction by an Isolated Monoalumoxane Anion. *Angew. Chem. Int. Ed.* **2019**, *58*, 18261–18265. [[CrossRef](#)]
73. Cui, C.; Roesky, H.W.; Schmidt, H.-G.; Noltemeyer, M. $[\text{HC}\{\text{(CMe)(NAr)}\}_2\text{Al}\{\text{(NSiMe}_3)_2\text{N}_2\}]$ (Ar = 2,6- $\text{iPr}_2\text{C}_6\text{H}_3$): The First Five-Membered AlN_4 Ring System. *Angew. Chem. Int. Ed.* **2000**, *39*, 4531–4533. [[CrossRef](#)]
74. Hicks, J.; Vasko, P.; Goicoechea, J.M.; Aldridge, S. The Aluminyl Anion: A New Generation of Aluminium Nucleophile. *Angew. Chem. Int. Ed.* **2020**, *60*, 1702–1713. [[CrossRef](#)]
75. Hicks, J.; Heilmann, A.; Vasko, P.; Goicoechea, J.M.; Aldridge, S. Trapping and Reactivity of a Molecular Aluminium Oxide Ion. *Angew. Chem. Int. Ed.* **2019**, *58*, 17265–17268. [[CrossRef](#)] [[PubMed](#)]
76. Dodonov, V.A.; Kushnerova, O.A.; Rummyantsev, R.V.; Novikov, A.S.; Osmanov, V.K.; Fedushkin, I.L. Cycloaddition of isoselenocyanates to sodium and magnesium metallacycles. *Dalton Trans.* **2022**, *51*, 4113–4121. [[CrossRef](#)] [[PubMed](#)]
77. Zhang, W.; Dodonov, V.A.; Chen, W.; Zhao, Y.; Skatova, A.A.; Fedushkin, I.L.; Roesky, P.W.; Wu, B.; Yang, X.-J. Cycloaddition versus Cleavage of C=S Bond of Isothiocyanates Promoted by Digallane Compounds with Non-Innocent α -Diimine Ligands. *Chem. Eur. J.* **2018**, *24*, 14994–15002. [[CrossRef](#)] [[PubMed](#)]
78. Fedushkin, I.L.; Moskalev, M.V.; Lukoyanov, A.N.; Tishkina, A.N.; Baranov, E.V.; Abakumov, G.A. Dialane with a Redox-Active Bis-amido Ligand: Unique Reactivity towards Alkynes. *Chem. Eur. J.* **2012**, *18*, 11264–11276. [[CrossRef](#)]
79. Feng, Z.; Liu, X.; Wang, Y.; Meng, C. Recent Advances on Gallium-Modified ZSM-5 for Conversion of Light Hydrocarbons. *Molecules* **2021**, *26*, 2234. [[CrossRef](#)]
80. Feng, Z.; Liu, X.; Meng, C. Speciation and interconversion of atomically dispersed extra-framework Ga in ZSM-5 zeolite. *Appl. Surf. Sci.* **2023**, *636*, 157811. [[CrossRef](#)]
81. Dmitrienko, A.; Pilkington, M.; Nikonov, G.I. Selective Cross-Coupling of Unsaturated Substrates on AlI. *Chem. Eur. J.* **2021**, *27*, 5730–5736. [[CrossRef](#)]
82. Roy, M.M.D.; Heilmann, A.; Ellwanger, M.A.; Aldridge, S. Generation of a π -Bonded Isomer of $[\text{P}_4]^{4-}$ by Aluminyl Reduction of White Phosphorus and its Ammonolysis to PH_3 . *Angew. Chem. Int. Ed.* **2021**, *60*, 26550–26554. [[CrossRef](#)]
83. Kong, R.Y.; Crimmin, M.R. Reversible insertion of CO into an aluminium–carbon bond. *Chem. Commun.* **2019**, *55*, 6181–6184. [[CrossRef](#)]
84. Hicks, J.; Vasko, P.; Goicoechea, J.M.; Aldridge, S. Reversible, Room-Temperature C–C Bond Activation of Benzene by an Isolable Metal Complex. *J. Am. Chem. Soc.* **2019**, *141*, 11000–11003. [[CrossRef](#)] [[PubMed](#)]
85. Boronski, J.T.; Thomas-Hargreaves, L.R.; Ellwanger, M.A.; Crumpton, A.E.; Hicks, J.; Bekiş, D.F.; Aldridge, S.; Buchner, M.R. Inducing Nucleophilic Reactivity at Beryllium with an Aluminyl Ligand. *J. Am. Chem. Soc.* **2023**, *145*, 4408–4413. [[CrossRef](#)] [[PubMed](#)]
86. Dodonov, V.A.; Xiao, L.; Kushnerova, O.A.; Baranov, E.V.; Zhao, Y.; Yang, X.-J.; Fedushkin, I.L. Transformation of carbodiimides to guanidine derivatives facilitated by gallylenes. *Chem. Commun.* **2020**, *56*, 7475–7478. [[CrossRef](#)] [[PubMed](#)]
87. Dodonov, V.A.; Kushnerova, O.A.; Baranov, E.V.; Novikov, A.S.; Fedushkin, I.L. Activation and modification of carbon dioxide by redox-active low-valent gallium species. *Dalton Trans.* **2021**, *50*, 8899–8906. [[CrossRef](#)] [[PubMed](#)]
88. Fedushkin, I.L.; Lukoyanov, A.N.; Tishkina, A.N.; Fukin, G.K.; Lyssenko, K.A.; Hummert, M. Reduction of digallane $[(\text{dpp-bian})\text{Ga-Ga}(\text{dpp-bian})]$ with Group 1 and 2 metals. *Chem. Eur. J.* **2010**, *16*, 7563–7571. [[CrossRef](#)] [[PubMed](#)]

89. Chen, M.-T.; Huang, C.-A.; Chen, C.-T. Palladacyclic Complexes Containing C,N-Type Ligands as Catalysts in Cross-Coupling Reactions. *Eur. J. Inorg. Chem.* **2008**, *2008*, 3142–3150. [[CrossRef](#)]
90. Delebecq, E.; Pascault, J.-P.; Boutevin, B.; Ganachaud, F. On the Versatility of Urethane/Urea Bonds: Reversibility, Blocked Isocyanate, and Non-isocyanate Polyurethane. *Chem. Rev.* **2013**, *113*, 80–118. [[CrossRef](#)] [[PubMed](#)]
91. Saunders, J.H.; Slocombe, R.J. The Chemistry of the Organic Isocyanates. *Chem. Rev.* **1948**, *43*, 203–218. [[CrossRef](#)]
92. Yamamoto, Y.; Yamazaki, H. Low-valent isocyanide complexes and clusters of palladium and platinum. Crystal structure of $[Pt\{C(=NR)N(R)C(=NR)(RNC)_2\}(R = 2,6-Me_2C_6H_3)]$. *J. Chem. Soc. Dalton Trans.* **1989**, *1989*, 2161–2166. [[CrossRef](#)]
93. Riera, V.; Ruiz, J.; Tiripicchio, A.; Camellini, M.T. Synthesis of coordinated carbon monoxide from isocyanide iron(II) compounds. Crystal structure of $[Fe(dppe)(CO)(CN-p-tol)(p-tolN=C-N-p-tol-C=N-p-tol)]$. *J. Organomet. Chem.* **1987**, *327*, C5–C8. [[CrossRef](#)]
94. Hoberg, H.; Oster, B.W.; Krüger, C.; Tsay, Y.H. Nickela-heteroringe aus nickel(0) und phenylisocyanat. *J. Organomet. Chem.* **1983**, *252*, 365–373. [[CrossRef](#)]
95. Paul, F.; Fischer, J.; Ochsenbein, P.; Osborn, J.A. Syntheses, interconversions and reactivity of heteropalladacycles made from aryl isocyanates and various phenanthroline Pd(II) precursors with small molecules. *Comptes Rendus Chim.* **2002**, *5*, 267–287. [[CrossRef](#)]
96. Lam, H.-W.; Wilkinson, G.; Hussain-Bates, B.; Hursthouse, M.B. Reactions of tert-butyl isocyanate and trimethylsilyl azide with imidoamido compounds of chromium, molybdenum and tungsten. *J. Chem. Soc. Dalton Trans.* **1993**, *1993*, 781–788. [[CrossRef](#)]
97. Weber, L.; Lassahn, U.; Stammer, H.-G.; Neumann, B. Inversely Polarized Phosphaalkenes as Phosphinidene- and Carbene-Transfer Reagents. *Eur. J. Inorg. Chem.* **2005**, *2005*, 4590–4597. [[CrossRef](#)]
98. Cui, C.; Köpke, S.; Herbst-Irmer, R.; Roesky, H.W.; Noltemeyer, M.; Schmidt, H.-G.; Wrackmeyer, B. Facile Synthesis of Cyclopropene Analogues of Aluminum and an Aluminum Pinacolate, and the Reactivity of $LAl[\eta^2-C_2(SiMe_3)_2]$ toward Unsaturated Molecules ($L = HC[(CMe)(NAr)]_2$, $Ar = 2,6-i-Pr_2C_6H_3$). *J. Am. Chem. Soc.* **2001**, *123*, 9091–9098. [[CrossRef](#)] [[PubMed](#)]
99. Fedushkin, I.L.; Skatova, A.A.; Cherkasov, V.K.; Chudakova, V.A.; Dechert, S.; Hummert, M.; Schumann, H. Reduction of Benzophenone and 9(10H)-Anthracenone with the Magnesium Complex $[(2,6-iPr_2C_6H_3-bian)Mg(thf)_3]$. *Chem. Eur. J.* **2003**, *9*, 5778–5783. [[CrossRef](#)] [[PubMed](#)]
100. Fachinetti, G.; Biran, C.; Floriani, C.; Chiesi Villa, A.; Guastini, C. C:O and C:C bond activation in diphenylketene promoted by dicarbonylbis(eta-cyclopentadienyl)titanium(II). *Inorg. Chem.* **1978**, *17*, 2995–3002. [[CrossRef](#)]
101. Evans, W.J.; Drummond, D.K. Reductive coupling of pyridazine and benzaldehyde azine and reduction of bipyridine by samarium complex $(C_5Me_5)_2Sm(THF)_2$. *J. Am. Chem. Soc.* **1989**, *111*, 3329–3335. [[CrossRef](#)]
102. Ohff, A.; Zippel, T.; Arndt, P.; Spannenberg, A.; Kempe, R.; Rosenthal, U. Reactions of Azines with Titanocene: C-H Activation, C-C Coupling, and N-N Cleavage to Heterobimetallic Complexes. *Organometallics* **1998**, *17*, 1649–1651. [[CrossRef](#)]
103. Fedushkin, I.L.; Lukoyanov, A.N.; Fukin, G.K.; Ketkov, S.Y.; Hummert, M.; Schumann, H. Synthesis, Molecular Structure and DFT Study of $(dpp-bian)Ga-M(Et_2O)_3$ ($M = Li, Na$; $dpp-bian = 1,2-bis(2,6-diisopropylphenyl)imino acenaphthene$). *Chem. Eur. J.* **2008**, *14*, 8465–8468. [[CrossRef](#)] [[PubMed](#)]
104. Lee, S.; Kim, T.H.; Shin, Y.W.; Jeon, Y.; Kim, J. Amitraz. *Acta Crystallogr. Sect. E* **2013**, *69*, o1300. [[CrossRef](#)] [[PubMed](#)]
105. Carugo, O.; Poli, G.; Manzoni, L. Structure of N,N',N'' -triphenylbiuret. *Acta Crystallogr. Sect. C* **1992**, *48*, 2013–2016. [[CrossRef](#)]
106. Ghosh, R.; Samuelson, A.G. Catalytic metathesis of carbon dioxide with heterocumulenes mediated by titanium isopropoxide. *Chem. Commun.* **2005**, *2005*, 2017–2019. [[CrossRef](#)] [[PubMed](#)]
107. Hardman, N.J.; Power, P.P. Dimeric Gallium Oxide and Sulfide Species Stabilized by a Sterically Encumbered β -Diketiminato Ligand. *Inorg. Chem.* **2001**, *40*, 2474–2475. [[CrossRef](#)] [[PubMed](#)]
108. Lide, D.R. *CRC Handbook of Chemistry and Physics*, 90th ed.; CD-ROM Version 2010; CRC Press/Taylor and Francis: Boca Raton, FL, USA, 2010.
109. Wang, X.M.; Fan, R.Q.; Qiang, L.S.; Li, W.Q.; Wang, P.; Zhang, H.J.; Yang, Y.L. Tunable luminescence from rare 2D Ga(III)/In(III) coordination polymers coexisting with three different conjugated system aromatic ligands. *Chem. Commun.* **2014**, *50*, 5023–5026. [[CrossRef](#)] [[PubMed](#)]
110. Cordero, B.; Gomez, V.; Platero-Prats, A.E.; Reyes, M.; Echeverria, J.; Cremades, E.; Barragan, F.; Alvarez, S. Covalent radii revisited. *Dalton Trans.* **2008**, *2008*, 2832–2838. [[CrossRef](#)]
111. Arii, H.; Amari, T.; Kobayashi, J.; Mochida, K.; Kawashima, T. Low-Coordinate Germanium(II) Centers Within Distorted Axially Chiral Seven-Membered Chelates: Stereo- and Enantioselective Cycloadditions. *Angew. Chem. Int. Ed.* **2012**, *51*, 6738–6741. [[CrossRef](#)]
112. Mom, V.; de With, G. A reinvestigation on benzalazine, influence of TDS and comparison with different experiments. *Acta Crystallogr. Sect. B* **1978**, *34*, 2785–2789. [[CrossRef](#)]
113. Bruker APEX3. *Bruker Molecular Analysis Research Tool*; v. 2018.7-2; Bruker AXS: Madison, WI, USA, 2018.
114. *Data Collection, Reduction and Correction Program*; CrysAlisPro 1.171.40.67a—Software Package; Rigaku OD: Tokyo, Japan, 2019.
115. Bruker. *SAINT Data Reduction and Correction Program v. 8.40B*; Bruker AXS: Madison, WI, USA, 2019.
116. Sheldrick, G.M. *SADABS v.2016/2, Bruker/Siemens Area Detector Absorption Correction Program*; Bruker AXS: Madison, WI, USA, 2016.
117. Krause, L.; Herbst-Irmer, R.; Sheldrick, G.M.; Stalke, D. Comparison of silver and molybdenum microfocus X-ray sources for single-crystal structure determination. *J. Appl. Crystallogr.* **2015**, *48*, 3–10. [[CrossRef](#)]
118. *SCALE3 ABSPACK: Empirical Absorption Correction*; CrysAlisPro 1.171.40.67a—Software Package; Rigaku OD: Tokyo, Japan, 2019.

119. Farrugia, L. WinGX and ORTEP for Windows: An update. *J. Appl. Crystallogr.* **2012**, *45*, 849–854. [[CrossRef](#)]
120. Sheldrick, G. SHELXT—Integrated space-group and crystal-structure determination. *Acta Crystallogr. Sect. A* **2015**, *71*, 3–8. [[CrossRef](#)] [[PubMed](#)]
121. Sheldrick, G.M. *SHELXTL. Structure Determination Software Suite*; Version 6.14; Bruker AXS: Madison, WI, USA, 2003.
122. Sheldrick, G. Crystal structure refinement with SHELXL. *Acta Crystallogr. Sect. C* **2015**, *71*, 3–8. [[CrossRef](#)] [[PubMed](#)]
123. Dolomanov, O.V.; Bourhis, L.J.; Gildea, R.J.; Howard, J.A.K.; Puschmann, H. OLEX2: A complete structure solution, refinement and analysis program. *J. Appl. Crystallogr.* **2009**, *42*, 339–341. [[CrossRef](#)]

Disclaimer/Publisher’s Note: The statements, opinions and data contained in all publications are solely those of the individual author(s) and contributor(s) and not of MDPI and/or the editor(s). MDPI and/or the editor(s) disclaim responsibility for any injury to people or property resulting from any ideas, methods, instructions or products referred to in the content.